p-ISSN: 1410-6957, e-ISSN: 2503-5029
https://jurnal.batan.go.id/index.php/ganendra

IMPROVEMENT OF ARJUNA 1.0 CONVEYOR SYSTEM FOR 3D IRRADIATION

PENINGKATAN SISTEM KONVEYOR ARJUNA 1.0 UNTUK IRADIASI 3D

Saefurrochman[1,*], Agus Tri Purwanto[1], Suhadah Rabi'atul Adabiah[1], Sukaryono[1], Galih Setiaji[1], Dwi Handoko Arthanto[1], Karina Anggraeni[1], Isti Dian Rachmawati[1], Agus Dwiatmaja[1], Wijono[1], Elin Nuraini[1], Wiwien Andriyanti[1], Darsono[1], Andreas Bimo Putro Adjie[2]

[1]Research Center for Accelerator Technology, Research Organization for Nuclear Technology, Kawasan Puspiptek Serpong, Tangerang Selatan, 15340

[2]Department of Mechanical and Industrial Engineering, Gadjah Mada University, Jl. Grafika No. 2 Yogyakarta, 55281

*Corresponding author e-mail: saef005@brin.go.id

Received 3 March 2023, revised 13 July 2023, accepted 28 July 2023

ABSTRACT

IMPROVEMENT OF ARJUNA 1.0 CONVEYOR SYSTEM FOR 3D IRRADIATION. *Design improvement of the conveyor system of Arjuna 1.0 electron accelerator for 3D object irradiation has been done. The penetration of electrons is less than 1 cm in the surface, causing a challenge for the irradiation process for sterilization of 3D objects. We designed a conveyor that can be rotated 360° to irradiate objects evenly. The dimension of this conveyor is 1750 x 600 x 800 mm and the maximum diameter of the object is 7 cm. Based on the Frame Bending Stress analysis to calculate the strength of the conveyor frame, it is shown that the maximum displacement is only 0.029 mm, which is very small so it will cause no disturbance to power transfer from the motor to the conveyor. The normal stress (Smax) is 3.926 MPa, and the bending stress for Smax (Mx) and Smax (My) are 2.391 MPa and 3.925 MPa, respectively. We also calculated the stress analysis of the 3 mm-thickness of the motor mount and found that the Von-Misses Stress, the first and third Principal Stress are 4.425 MPa, 5.01 MPa, and 1.95 MPa, respectively. These results confirm that the design and the material used for the conveyor are safe because the stress is very low than the material yield strength of 207 MPa. The needed power for this conveyor is 0.01724 kW, with a maximum speed is 880 rpm. The new model of a 3D conveyor has been constructed and can be implemented to ARJUNA 1.0 to irradiate objects on all its surfaces.*

Keywords*: 3D irradiation, conveyor system, stress analysis*

ABSTRAK

PENINGKATAN SISTEM KONVEYOR ARJUNA 1.0 UNTUK IRADIASI 3D. *Pengembangan desain sistem konveyor akselerator elektron Arjuna 1.0 untuk iradiasi objek 3D telah dilakukan. Penetrasi elektron berenergi rendah kurang dari 1 cm di permukaan, menyebabkan tantangan bagi proses iradiasi untuk sterilisasi objek 3D. Kami merancang konveyor yang dapat diputar 360° untuk mengiradiasi objek secara merata. Dimensi konveyor ini adalah 1750 x 600 x 800 mm dan diameter maksimum objek adalah 7 cm. Berdasarkan analisis Frame Bending Stress untuk menghitung kekuatan rangka konveyor, terlihat perpindahan maksimal hanya 0,029 mm yang sangat kecil sehingga tidak akan menimbulkan gangguan perpindahan daya dari motor ke konveyor. Normal stress (Smax) adalah 3,926 MPa, bending stress untuk Smax (Mx) dan Smax (My) masing-masing adalah 2,391 MPa dan 3,925 MPa. Kami juga menghitung analisis tegangan dengan ketebalan 3 mm dari dudukan motor dan menemukan bahwa Stres Von-Misses, Stres Utama pertama, dan ketiga masing-masing adalah 4,425 MPa, 5,01 MPa, dan 1,95 MPa. Hasil ini menegaskan bahwa desain dan material yang digunakan untuk conveyor aman karena tegangannya sangat rendah dari yield strength material yaitu 207 MPa. Daya yang dibutuhkan untuk konveyor ini adalah 0, 01724 kW, dengan kecepatan maksimum sebesar 880 rpm. Model baru konveyor 3D telah dibangun dan dapat diimplementasikan ke ARJUNA 1.0 untuk mengiradiasi objek di seluruh permukaannya.*

Kata kunci*: iradiasi 3D, sistem konveyor, analisis stress*

INTRODUCTION

One of the difficulties of irradiation using low-energy electron accelerators is their low penetration on the material surface [1]. The electron beam penetration for a 350 keV accelerator is only around 0.75 mm [2], measured by cellulose triacetate (CTA) dosimeter. The penetration depth which is less than 1 cm, makes the irradiation process for the sterilization of 3D objects difficult, time-consuming, and non-effective. Therefore, it is necessary to improve the irradiation system, making the irradiation process more productive and efficient.

https://doi.org/10.55981/gnd.2023.6826

In the irradiation process using an electron beam, the distance between the window and the object is very important because the electron can interact with oxygen in the air and produce ozone. This leads to electron beam loss and reduces electron intensity before it hits the target. Other disadvantages are that the conventional conveyor (Fig. 1) cannot be moved freely because of its heavy weight, and vertical movement to adjust the height of the conveyor (distance between window and target) is also not possible [3]. It makes an inefficient process of irradiation.

Figure 1. Conveyor system for irradiation in Arjuna 1.0

Conveyors are part of a considerably larger group of equipment used for material handling [4]. The manual handling of materials is typically decreased or eliminated with the proper use of material-handling equipment [5]. Engineers have developed a variety of operating systems and mechanisms for conveyors as a result of the expansion of their applications and the use of new technologies, but in general, most conveyors use an electromotor to move an axis that is primarily a drum, a cylinder that moves a belt by friction (attached to it) [5]. On the other hand, the rolling drum creates a loop using a belt or chain that may be moved from one location to another by putting materials or things [6]. There are several types of conveyors, including gravity roller conveyors, chain conveyors, bucket elevators, conveyor rollers, and ground conveyors [7].

Until now, the irradiation system in Arjuna 1.0 accelerator electron only uses a 2-dimensional irradiation system[8]. It means that the object can be irradiated only on one surface at the time so the applications are limited to surface coating, crosslinking processes such as batik irradiation [9], latex vulcanization [10], and other surface irradiation processes [11]. The current irradiation system uses a fixed roller conveyor that moves objects at various speeds. However, the design of this conventional conveyor is fixed and the movement is limited to horizontal movement [12].

Many studies about the design and optimization of conveyor system have been conducted. Bhavesh et.al. designed and tested a novel screw conveyor-based system to scoop crude oil sludge from the floor of oil storage tanks. This proposed new system consists of a screw conveyor mounted on a 'C' shaped casing with a bearing on both sides driven by a waterproof motor through a worm drive [13]. M.L. Dezaki, et al.[14] also designed a new type of conveyor, electropneumatic conveyor belt robots with two separated lines. Its unique feature is a combination of various systems to develop an electropneumatic robot. They designed and developed an automated and intelligent mechatronic conveyor system for transporting and positioning circular objects that can be used in the manufacturing and packaging industries. Zhang, et al. [7] also made some improvements in the energy efficiency of belt conveyor systems. The improvement of variable speed control is important to develop the operation efficiency of belt conveyors. Six optimization problems of a typical belt conveyor system were formulated with solutions in simulation for a case study.

However, the study of a conveyor system that can rotate 360° in order to irradiate the surface of an object maximally is still a few. In this study, we proposed a new type of irradiation transport system using 3D conveyor with rotation of 360° which can irradiate objects on all its surface. Thus, it is expected to reduce costs, time, and energy consumption. In addition, this new type of conveyor also can simplify the installation, improve the environment, and increase the efficiency of the irradiator process. The purpose of this work specifically is to design the 3D conveyor for fruit sterilization to kill the bacteria, insects, and many parasites on its surface to enhance their time-preserving. However, this conveyor is not limited only to fruit, but also to another object with a maximum diameter of 7 cm. The conveyor system consists of mechanical and instrumentation systems however we limited

the discussion only about the mechanical system of the conveyor including the mechanical drawing, stress analysis, and calculation of the needed power to run the system.

METHODOLOGY

The research started with the study of the needs for conveyor systems in electron beam machine. The dimensions of the room and the window, and the distance between the window and the needed conveyor were measured. Then, modeling and designing of the conveyor system including 2-dimensional and 3-dimensional drawings were carried out. The conveyor was designed using Autodesk Inventor 2020 software with a student license. Moreover, frame analysis and stress analysis are also performed by this software. The next step was to determine the material of each component. Then, the needed motor power was calculated to run the system. The last is to simulate frame analysis and stress analysis. The components of the conveyor system are listed in Table 1. Modeling was carried out using Autodesk Inventor and obtained the design, as shown in Fig. 2.

Stress analysis is a structural analysis method using the concept of Finite Element Analysis (FEA) [15]. This analysis concept is to divide the workpiece into small elements with finite numbers connected to each other to calculate at each point of the element. The FEA is divided into three steps, namely, preprocessing, meshing, and post-processing.

Frame Analysis is a frame structure analysis method that is a feature in Autodesk Inventor software. The concept of this analysis is to apply the science of structural mechanics, such as the shear force diagram (SFD) which shows the variation of shear force along the length of the beam, the bending moment diagram (BMD) which shows the variation of bending moment along the length of the beam, a normal force diagram (NFD) and other calculations related to beams, frames, and trusses. Just like stress analysis, data such as boundary conditions, forces and working moments, pedestals, geometry, and materials of the structure used must be entered first for calculation by a computer.

The characteristics observed from stress and frame analysis [16] are displacement, normal stress, principal stress, bending stress, and Von-Misses stress. Displacement is the shift of a certain point when receiving a load compared to the initial position. Normal stress is the stress that occurs when the applied force is perpendicular to the tension surface. Principal stress is an extreme value of the normal stress experienced by the material. There are 2 types of principal stress, namely first that accommodates tensile force and the third that provides compressive force. Bending stress is the stress caused by normal stress (with different directions and magnitudes at different points) that causes the object to bend. Von-Misses Stress is the sum of all stress experienced by a frame derived from the principal axis and related to principal stress. This is important because at very minimal, even zero costs, the reaction of a structure or component to a particular force, moment, or condition can be predicted with a high degree of accuracy (depending on the settings).

Table 1. New type components of conveyor system

Components	Dimension	Material
Table Frame	1750 × 600 × 800 mm	Elbow iron/angle bar 50 × 50 × 4 mm
Motor mounting plate	588 × 362 × 3 mm	3 mm thick iron plate
Housing	outer diameter 112 mm and length 65 mm	SS 304 127 mm in diameter
Vessel cover	outer diameter 90 mm, inner diameter 80 mm, and width 20 mm	SS 304
Middle flange	outer diameter 110 mm, inner diameter 80 mm, and width 16 mm	SS 304
Banners	4 mm in diameter	SS 304
Housing bottom bracket	250 × 150 mm	SS 304 20 mm thick
Housing top bracket	250 × 130 mm	SS 304 20 mm thick
Right and Left Pipe Brackets	90 × 65.96 × 61.75 mm	SS 201
AC and VFD motors	3-phase electric motor	3-phase electric motor
Edge pipe brackets	130 × 71.75 × 25 mm	SS 201

In this new design (see Fig. 2), the fruits or objects to be irradiated have a round shape with a diameter less than the conveyor diameter. Therefore, even though the conveyor system only serves 1 degree of rotational freedom, the objects can be irradiated evenly. The conveyor will be placed right under the window where the distance between the conveyor and the window is 20 cm. The length of the conveyor is as long as the window length, which is 120 cm, so the conveyor is placed in a horizontal position under the window. The irradiated area is

 https://doi.org/10.55981/gnd.2023.6826

expected to be larger with this installation compared to the vertical installation like the old conveyor, shown in Fig. 1.

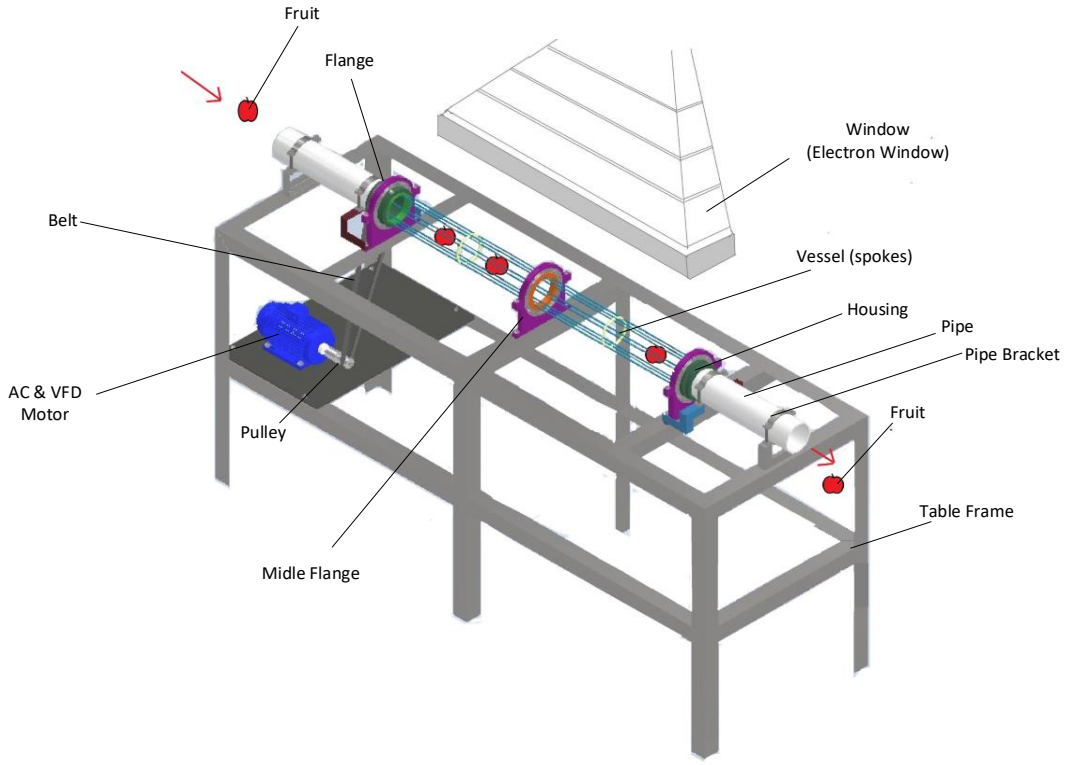

Figure 2. Conveyor system assembly for 3D irradiation

The conveyor system contains several parts with different functions. The housing functions as one of the vessel components that will continue the rotation from the belt to the vessel (acting as one of the pulleys) and hold the vessel cover component. The vessel cover holds the end of the spokes and connects it with the housing. The middle flange serves as one of the components of the support of the vessel spokes right in the middle. The spokes serve as a vessel wall that will be rotated and limit or direct the movement of the fruit as it passes through the vessel. The lower bracket of the housing serves as one of the fastening components of the housing on the lower side and becomes a mount for the bearing on the outer side. The upper bracket of the housing serves as one of the fastening components of the housing on the upper side and the bearing on the outer side. The right and left pipe brackets act to ensure that PVC pipes (fruit inlets and outlets) remain on one axis with vessels. The shaft motor runs to pass power from the motor to the bottom pulley.

Pulley-Belt System Design and Calculation

The pulley and belt behave as a power-forwarding mechanism from the motor to the vessel. The pulley has an outermost diameter of 30 mm, the smallest diameter (hole) of 6 mm, and an overall length of 30 mm which is made of aluminum axles of 0.75 inch (44.45 mm) in diameter. Then, the axles are bolted to form a design-like profile. The key path profiles can be made with a scrap machine or a slotter machine. Meanwhile, the belts can be purchased in the marketplace.

The size of the used pulley can be determined through the calculations in Eq.1[17]:

$$D_{pk} = \frac{\omega pb \; x \; Dpb}{\omega pk} \qquad (1)$$

where D_{pk} is the small pulley diameter (mm), D_{pb} is the big pulley diameter (mm), ωpb is the angular velocity of the big pulley (rpm), and ωpk is the angular velocity of small pulley (rpm). By inputting these values into Eq. 1, i.e. motor speed of 880 rpm, vessel speed of 200 rpm, large pulley size (housing) of 110 mm, and small pulley size (motor), so the small pulley diameter can be obtained as:

$$D_{pk} = \frac{200\ rpm\ x\ 110\ mm}{880\ rpm} = 25\ mm$$

If the motor is placed in the middle, the used belt size can be determined through the calculation using Eq. (2)

$$L = (2C) + \left(1{,}57(D1 + D2)\right) + \frac{(D2-D1)^2}{4C} \qquad (1)$$

where *L* is the belt length (mm), *C* is the distance between the pulley (445 mm), *D1* is the big pulley diameter (110 mm), and *D2* is the small pulley diameter (25 mm). The calculation of the belt length served using Eq. (2) is:

$$L = (2x445) + \left(1{,}57(110 + 25)\right) + \frac{(25-110)^2}{4x445} = 1106\ mm$$

However, due to the limitation of the v-belt transmission feature on the used Autodesk Inventor, the position of the motor cannot be in the middle and causes the length of the belt used to be 1150 mm so that the belt size has to be 46 inch or 1168.8 mm.

Calculation of Load Sharing on the Table

The calculation of sharing load was carried out specifically on the table because it supported the entire conveyor system. The concept of the struggle is by determining the type and magnitude of the force received by the table part that supports other components. The weight of each component listed is taken from the iProperty of each component that has been calculated and provided by Autodesk Inventor. The corresponding data for fastening components such as bolts, nuts, and washers, is taken from the particulars provided by the seller or component provider. Meanwhile, load sharing needs to be calculated with the concept of SFD as in structural mechanics for components that extend along vessels and tables. The sharing loads on the frame can be seen in Table 2. The sharing load calculations were simulated using beam analysis software on the website mechanicalc.com/calculators/beam-analysis.

Table 2. Continuous Loading Conditions

Constraint			
Location	TX	TY	Rotation
0	Free	Fixed	Fixed
1750	Free	Fixed	Fixed
875	Fixed	Fixed	Fixed
320	Fixed	Fixed	Fixed
1430	Fixed	Fixed	Fixed

Load Distribution				
Type	Location 1 (mm)	Location 2 (mm)	W1 (N/mm)	W2 (N/mm)
Spokes	349	1401	-0,00791	-0,00791
Fruit	0	1750	-0,02	-0,02

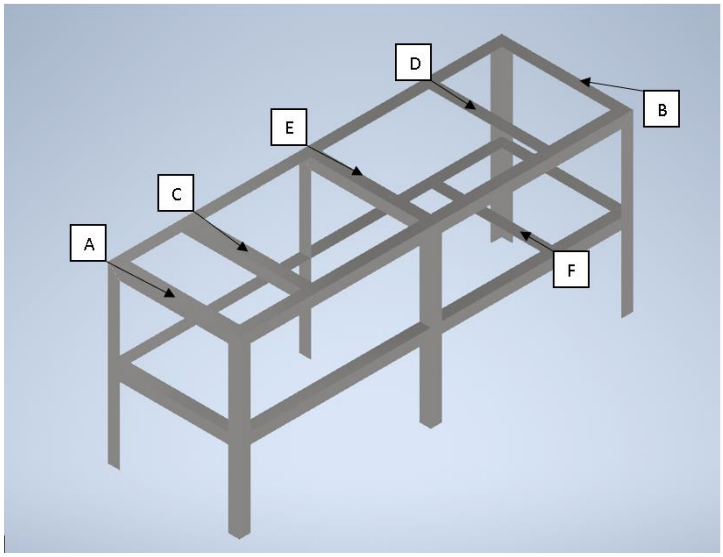

Figure 3. Location of Sharing Loads on Table Frame

https://doi.org/10.55981/gnd.2023.6826

Calculation of Motor Power Requirements

The electric motor is used to rotate the vessel so that the fruit can be turned and moved from the entry point to the outside point. The power requirement of the motor needs to be calculated as a factor determining the specifications of the motor. The first step is to calculate the mass inertia moment of the rotating components that will be moved by the motor. The components of the spokes and bolt housing, as well as the fruit that will later be irradiated treatment must be calculated manually because these do not rotate on the respective axes. The calculation of the inertia moment is considered to be the case of a tied ball at the end of the rope and a rotated ball at the other end of the rope. Then, the specific limit conditions were an initial speed of 0 rpm (rad/s), a maximum speed of 200 rpm (20.944 rad/s), and an acceleration time of 5 s. The angular acceleration at the heaviest condition can be calculated using (Eq. 3) [17]:

$$\alpha = \frac{\omega a - \omega o}{t} \qquad (3)$$

where α is the angular acceleration (rad/s^2), ωa is the final velocity (rad/s), ωo is the initial velocity (rad/s), and t is time (s). By inserting the values, the angular acceleration can be found using Eq. (3):

$$\alpha = \frac{(20{,}944-0)}{5} = 4{,}189\ rad/s^2$$

The equation of torque at the heaviest condition is

$$T = I\ x\ \alpha \qquad (2)$$

where T is torque (Nm) and I is inertia momentum (kg.m^2). Thus, the torque can be calculated by T = 0.01770 kg.m^2 x 4.189 rad/s^2 = 0.074121214 Nm. The equation of required motor power in the toughest conditions if the efficiency is 90% is

$$Pmax = eff\ x\ \frac{T\ x\ \omega\ x\ 2\pi}{6000} \qquad (3)$$

where eff is the system efficiency and $Pmax$ is the maximum power (kW). Hence, the required motor power was acquired at 0.01724 kW.

RESULTS AND DISCUSSIONS

In general, the design of the conveyor system of this fruit irradiation device is assembled by the vessels, fruit entrance, and exit paths, supporting tables, and drive systems. The working principle of such a vessel conveyor system is to rotate the vessel so that the workpiece in its path will be rotated and moved assisted by the push of other objects that enter the conveyor. The simulation results of load distribution on the frame are given in Fig. 4 and Fig. 5 for the fruit and flange's spokes, respectively.

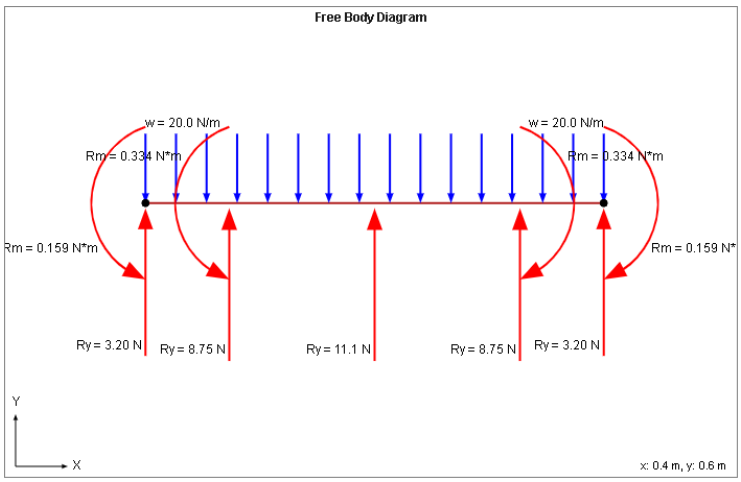

Figure 4. Fruit Continuous Loading Simulation Results

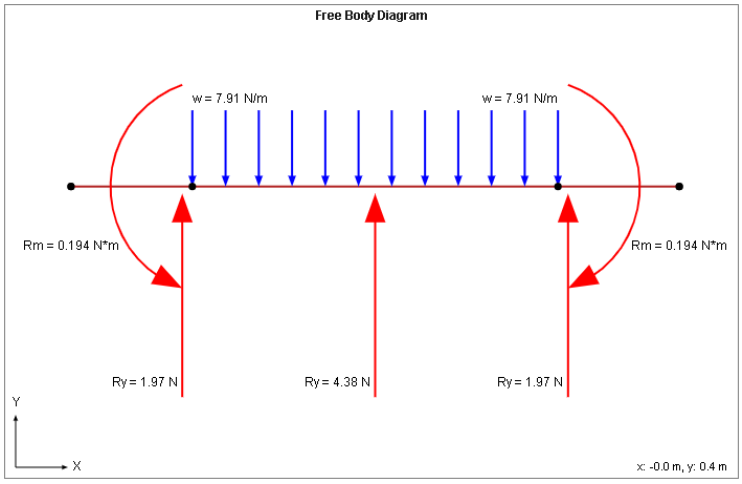

Figure 5. Simulation Results of Continuous Loading of Flange's Spokes

Frame Analysis of Table Frame

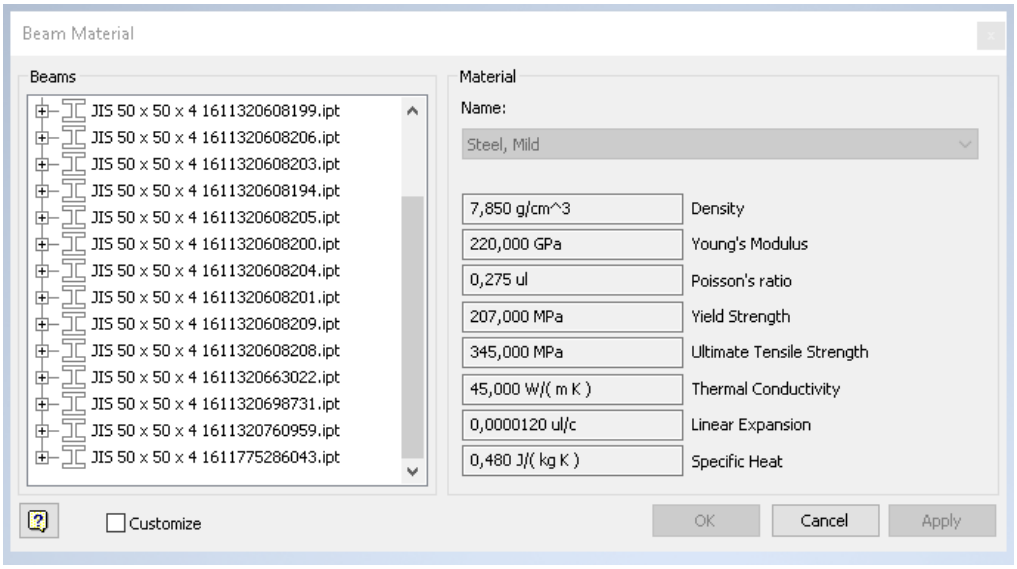

Figure 6. Table Frame Material Characteristics Data.

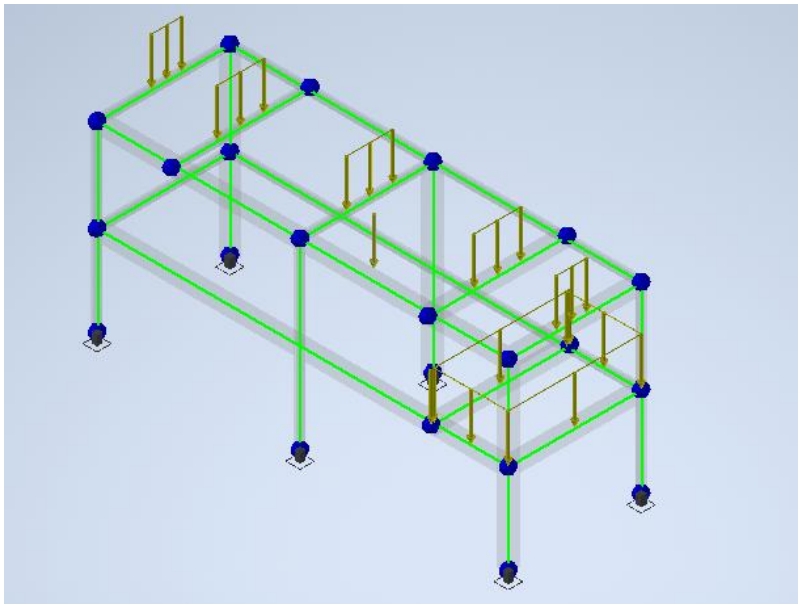

Figure 7. Loading Conditions and Constraint Frame Analysis

https://doi.org/10.55981/gnd.2023.6826

Frame analysis is carried out to determine the behavior of the frame in response to the force or moment that acts on the frame. The type of analysis is a static analysis. The table frame used elbow iron material with a profile of 50×50×4 mm which on Autodesk Inventor is represented with mild steel JIS G3192. Data on material characteristics can be seen in Fig. 6.

At the pre-processing step, the condition of the boundary or constraint is fixed supporting the six table legs that touch the ground. Then, the styles that work on the table were entered according to the data in Fig. 6. The selection of the continuous load type is based on the entire load being passed to the table frame through a flat and elongated bottom surface and the absence of pressure options on the Autodesk inventor. The weight of the table was also taken into account in this simulation. Loading conditions and constraints can be seen in Fig. 7.

Based on such characteristic data, boundary conditions, and load settings, the analysis results are listed in Table 3.

Table 3. Frame Analysis Result

Name		Minimum	Maximum
Displacement		0,000 mm	0,029 mm
Forces	Fx	-49,695 N	49,702 N
	Fy	-40,433 N	40,438 N
	Fz	-18,315 N	159,507 N
Moments	Mx	-5959,993 N mm	6622,995 N mm
	My	-6509,065 N mm	9786,230 N mm
	Mz	-44,985 N mm	45,216 N mm
Normal Stresses	Smax	-0,366 MPa	3,926 MPa
	Smin	-3,086 MPa	0,020 MPa
	Smax(Mx)	0,000 MPa	2,391 MPa
	Smin(Mx)	-2,656 MPa	-0,000 MPa
	Smax(My)	0,000 MPa	3,925 MPa
	Smin(My)	-2,611 MPa	-0,000 MPa
	Saxial	-0,410 MPa	0,047 MPa
Shear Stresses	Tx	-0,353 MPa	0,353 MPa
	Ty	-0,287 MPa	0,287 MPa
Torsional Stresses	T	-0,126 MPa	0,125 MPa

Name		Minimum	Maximum
Displacement		0,000 mm	0,029 mm
Forces	Fx	-49,695 N	49,702 N
	Fy	-40,433 N	40,438 N
	Fz	-18,315 N	159,507 N
Moments	Mx	-5959,993 N mm	6622,995 N mm
	My	-6509,065 N mm	9786,230 N mm
	Mz	-44,985 N mm	45,216 N mm
Normal Stresses	Smax	-0,366 MPa	3,926 MPa
	Smin	-3,086 MPa	0,020 MPa
	Smax(Mx)	0,000 MPa	2,391 MPa
	Smin(Mx)	-2,656 MPa	-0,000 MPa
	Smax(My)	0,000 MPa	3,925 MPa
	Smin(My)	-2,611 MPa	-0,000 MPa
	Saxial	-0,410 MPa	0,047 MPa
Shear Stresses	Tx	-0,353 MPa	0,353 MPa
	Ty	-0,287 MPa	0,287 MPa
Torsional Stresses	T	-0,126 MPa	0,125 MPa

Figs. 8 to 11 show that the largest displacement or displacement only reaches 0.029 mm (Fig. 9) which does not interfere with the mechanism of delivering power from the motor to the vessel conveyor. Then, all the stress that occurs in the frame, such as normal stress (SMax) in Fig. 10 of 3,926 MPa and bending stress (Smax (Mx) and Smax (My)) in Figs. 8 and 9 of 2,391 MPa and 3,925 MPa, is very far below the yield strength of the used material which reaches 207 MPa. It confirms that the design is safe to use.

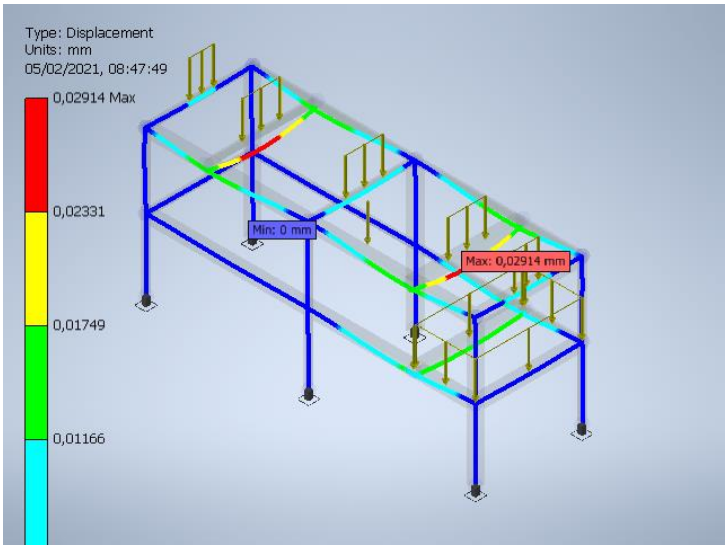

Figure 8. *Frame Displacement analysis result*

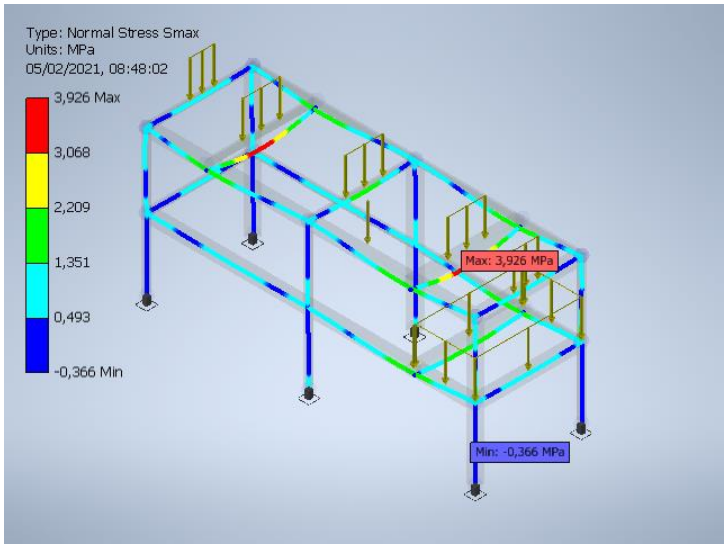

Figure 9. *Frame Normal Stress analysis result*

https://doi.org/10.55981/gnd.2023.6826

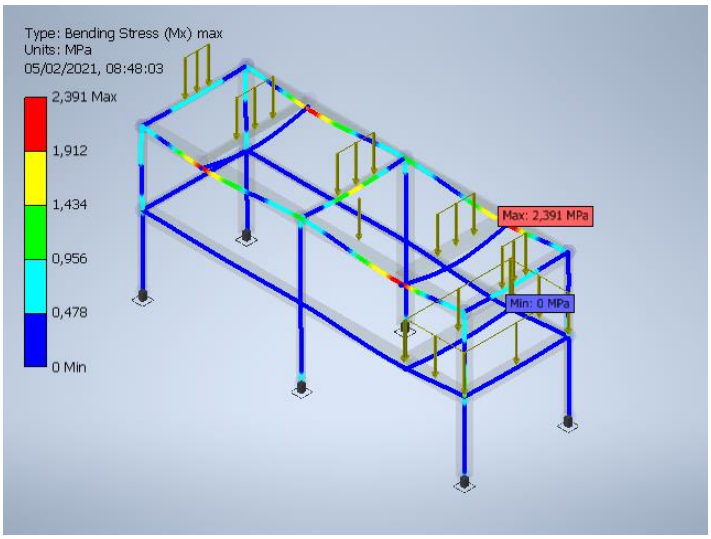

Figure 10. *Frame Bending Stress* X-direction analysis result

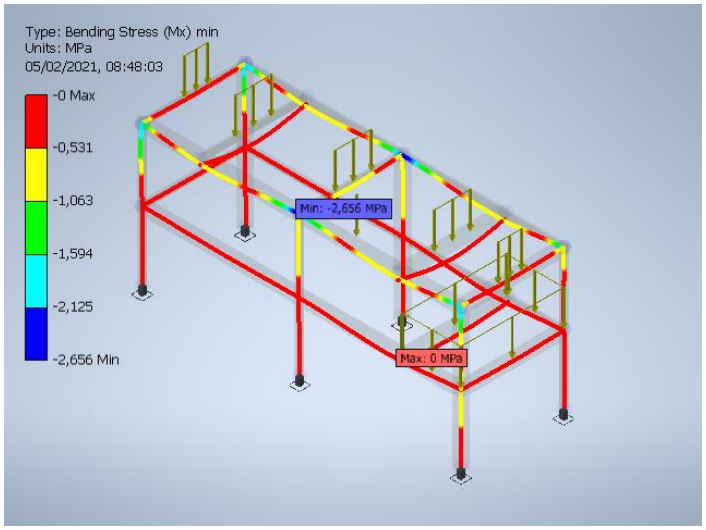

Figure 11. *Frame Bending Stress* in the Y-direction analysis result

Stress Analysis of Motor Mount Plate

Stress analysis is conducted to determine the behavior of the component, which is the motor mounting plate in this case, against the load acting on it. The type of performed analysis is static analysis. The motor mounting plate is made of a 3 mm thick machine plate which in Autodesk Inventor is represented with steel material.

At the pre-processing stage, the entered boundary condition is fixed which supports around the bottom of the plate with an offset of 44 mm from the outermost side of the plate because the plate contacts the surface of the table frame in this area (see Fig. 12). Then, the type of the entered load is a pressure of 0.005 MPa in the area where the electric motor is located. The weight of the plate is also taken into account. The setting of meshing used defaults of Autodesk Inventor.

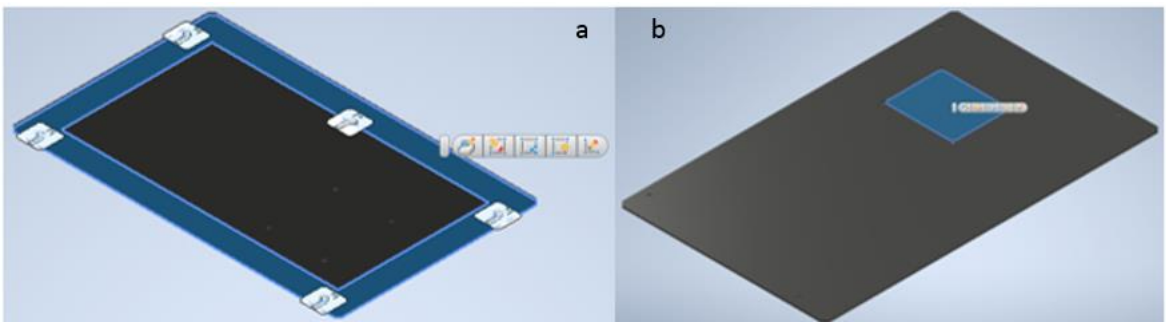

Figure 12. (a) Fixed Constraint dan (b) Contact area of Plat and Motor

Based on the characteristic data, boundary conditions, and such load settings, the analysis results are shown in Figs. 13 to 16. From the analysis results shown in Fig. 13, the Von-Misses stress only reached 4,425 MPa. The first and the third principal stress shown in Fig. 14 and Fig. 15, only reached 5.01 MPa and 1.95 MPa, respectively. These results are very far from the yield strength possessed by the plate material which reached 207 MPa. Hence, the use of a 3 mm thick plate is safe in this design. Based on Fig. 16, the displacement experienced by the plate only reaches 0.031 mm which is so small that it does not interfere with the power forwarding mechanism from the motor to the vessel conveyor.

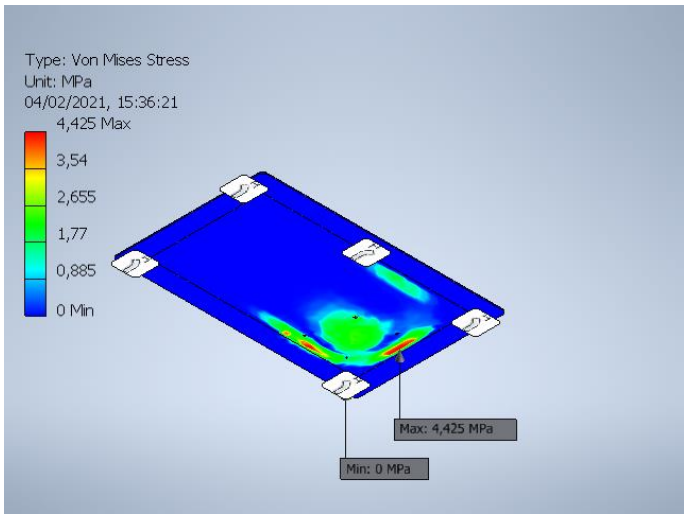

Figure 13. Von-Mises *Stress Analysis Result*

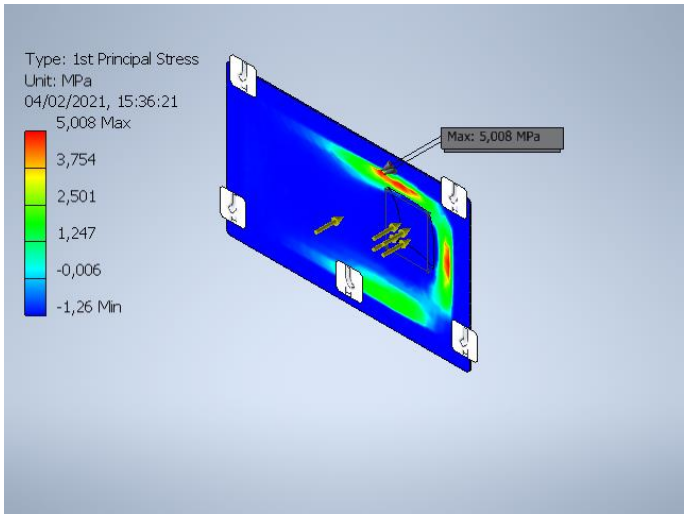

Figure 14. *First Principal Stress Analysis*

https://doi.org/10.55981/gnd.2023.6826

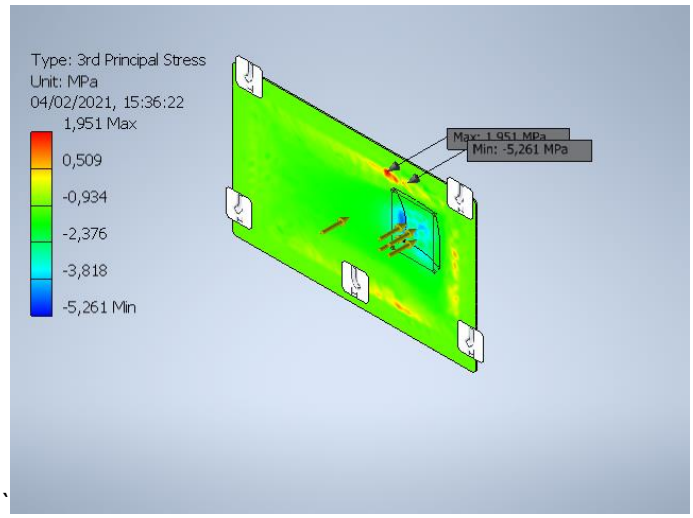

Figure 15. *Third Principal Stress Analysis*

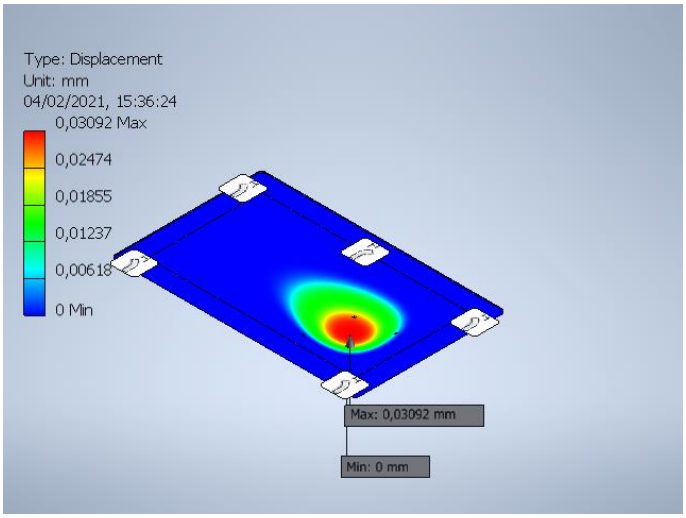

Figure 16. of *Stress Analysis-Displacement.*

CONCLUSION

The needed components in the conveyor system include a table frame, upper bracket housing, bracket under housing, housing, middle flange, vessel cover, right-left, and edge pipe brackets, spokes, shaft, pulley, PVC pipe clamps, AC motor, VFD, belt, shaft coupling, bearing, some fasteners, and fastening components. The table frame and motor mounting plate on the conveyor system work well and safely. All the analysis results which were carried out on the table frame and motor mounting plate showed that the voltages are far below the yield strength of the material. The required motor power in the conveyor system of the fruit irradiation device is 0.017240045 kW. After looking for its availability in the marketplace, the motor product was chosen 3-phase 6-pole electric motor with a power of 0.25 kW.

ACKNOWLEDGMENTS

Thank you to Mr. Suhartono and Mr. Sutadi for the technical consultation about Mechanical Structure.

REFERENCES

[1] D. S. Pudjorahardjo, “Aplikasi Mesin Berkas Elektron Di Pusat Teknologi Akselerator dan Proses Bahan - BATAN,” *Pertem. dan Present. Teknol. Akselerator dan Apl.*, vol. Edisi Khus, no. Juli, pp. 70–77, 2006, [Online]. Available: http://digilib.batan.go.id/e-prosiding/File Prosiding/Lingkungan/Ptapb_2006/data/Djoko SP 70-77.pdf

[2] S. Widodo *et al.*, “Policy review on research, development, and applications of particle accelerator in Indonesia,” *AIP Conf. Proc.*, vol. 2381, no. November, 2021, doi: 10.1063/5.0066284.

[3] BRIN, "Safety Analysis Report of Electron Beam Machine 300 keV/20 mA," Yogyakarta, 2021.

[4] P. Dąbek, P. Krot, J. Wodecki, P. Zimroz, J. Szrek, and R. Zimroz, "Measurement of idlers rotation speed in belt conveyors based on image data analysis for diagnostic purposes," *Meas. J. Int. Meas. Confed.*, vol. 202, no. June, p. 111869, 2022, doi: 10.1016/j.measurement.2022.111869.

[5] V. M. Patil, N. A. Vidya, R. L. Katkar, and P. S. Pande, "Type of Conveyor System: A Review," *IJSRD - International J. Sci. Res. Dev.*, vol. 2, no. 12, pp. 305–307, 2015.

[6] G. Fedorko *et al.*, "Failure analysis of belt conveyor damage caused by the falling material. Part I: Experimental measurements and regression models," *Eng. Fail. Anal.*, vol. 36, pp. 30–38, 2014, doi: 10.1016/j.engfailanal.2013.09.017.

[7] S. Zhang and X. Xia, "Modeling and energy efficiency optimization of belt conveyors," *Appl. Energy*, vol. 88, no. 9, pp. 3061–3071, 2011, doi: 10.1016/j.apenergy.2011.03.015.

[8] Saefurrochman, Darsono, S. R. Adabiah, E. Nuraini, Sutadi, and T. Ardiyati, "A NOVEL DESIGN OF 17.5 KV HV FEEDTHROUGH FOR ARJUNA 2.0 DESAIN," vol. e-ISSN: 25, no. p-ISSN: 1410-6957, p. 8, 2021, [Online]. Available: https://jurnal.batan.go.id/index.php/ganendra/article/download/6223/5444

[9] W. Andriyanti, D. Darsono, E. Nuraini, L. Indrayani, and M. Triwiswara, "Aplikasi Teknologi Mesin Berkas Elektron Pada Proses Pewarnaan Batik Katun Dengan Pewarna Alami Menggunakan Metode Curing," *GANENDRA Maj. IPTEK Nukl.*, vol. 23, no. 1, p. 39, 2020, doi: 10.17146/gnd.2020.23.1.5860.

[10] E. Nuraini, Darsono, W. Andriyanti, Saefurrochman, Sutadi, and S. R. Adabiah, "The effect of stirring speed variations on the mechanical properties of latex post- irradiation using the ARJUNA 1.0 electron beam," 2021, vol. 2381, 0200, p. 10.

[11] T. Abou Elmaaty, S. Okubayashi, H. Elsisi, and S. Abouelenin, "Electron beam irradiation treatment of textiles materials: a review," *J. Polym. Res.*, vol. 29, no. 4, 2022, doi: 10.1007/s10965-022-02952-4.

[12] A. H. Shali, Saminto, S. R. Adabiah, F. Lucyana, and Taufik, "Scanning Horn Simulation Code for Electron Beam Machine Based on Boris Algorithm," *Atom Indones.*, vol. 48, no. 3, pp. 205–213, 2022, doi: 10.17146/AIJ.2022.1186.

[13] B. Narayani, S. Ravichandran, and P. Rajagopal, "Design optimization of a novel screw conveyor based system to scoop oil sludge from floor of storage tanks," *Upstream Oil Gas Technol.*, vol. 6, no. December 2020, p. 100029, 2021, doi: 10.1016/j.upstre.2020.100029.

[14] M. L. Dezaki, S. Hatami, A. Zolfagharian, and M. Bodaghi, "A pneumatic conveyor robot for color detection and sorting," *Cogn. Robot.*, vol. 2, no. February, pp. 60–72, 2022, doi: 10.1016/j.cogr.2022.03.001.

[15] B. Setyono, "Perancangan Dan Analisis Kekuatan Frame Sepeda Hibrid 'Trisona' Menggunakan Software Autodesk Inventor," *J. IPTEK*, vol. 20, no. 2, p. 37, 2016, doi: 10.31284/j.iptek.2016.v20i2.43.

[16] M. P. Antartika, B. Budianto, M. Ari, and K. Suastika, "PERBANDINGAN HASIL ANALISIS METODE ELEMEN HINGGA BERBASIS SOFTWARE DENGAN SIMPLE SUPPORTED CALCULATION PADA KAPAL 50 PAX CRANE BARGE," *J. Integr.*, vol. 12, no. 1, pp. 72–78, 2020, doi: 10.30871/ji.v12i1.1451.

[17] V. B. Bhandari, *Design of Machine Elements Third Edition*. New Delhi: Tata McGraw-Hill Education Private Limited, 2010.